The Electron Cloud Effect: Summary

M. A. Furman
LBNL

Snowmass mtg. July 2001

PAC01: "smoking gun" evidence at many machines:
PEP-II, KEK-B, BEPC, APS, PSR, SPS, PS,
expected at LHC, possibly SNS

This talk builds on the experience of many people; I am particularly grateful to:

J. S. Berg, M. Blaskiewicz, O. Brüning, Y. Cai, I. Collins, A. Drees, O. Gröbner, K. Harkay, S. Heifets, N. Hilleret, R. Kirby, A. Kulikov, G. Lambertson, R. Macek, K. Ohmi, M. Pivi, J. Rogers, R. Rosenberg, J. Seeman, G. Stupakov, F. Zimmermann

The ECE in a nutshell:

1. beam produces electrons (PHOTOEMISSION, RESIDUAL GAS IONIZATION, PARTICLE LOSSES HITTING CHAMBER WALLS)
2. electrons get rattled around the chamber
   - from single-bunch passage, and/or
   - from multi-bunch passages
3. number of electrons may increase or decrease from collisions against the walls (SEY
4. electron cloud couple to the ~~protons~~ BEAM
   - within the bunch, and/or
   - successive bunches are coupled via the interbunch electron cloud

Especially strong effect for intense, positively-charged beams (e^+ or p); possible consequences:

- fast instability (single bunch or multibunch)
- emittance increase and/or particle losses
- excessive energy deposition on the walls (e.g., LHC)

In summary: the ECE is a consequence of the strong coupling between the beam and its environment;

- many ingredients: beam energy, bunch charge and spacing, photoelectric yield, photon reflectivity, secondary emission yield, chamber size and geometry, ...

BRIEF HISTORY OF E.C.E.

1977 : FIRST EVIDENCE ; BEAM-INDUCED MULTIPACTING (BIM) O. GRÖBNER , CERN (ISR , TESTING SAMPLE ALUMINUM CHAMBERS FOR ISABELLE)

- SUDDEN INCREASE IN VAC. PRESSURE (RESONANT ECE)

1995 : IZAWA , SATO , TOYOMASU (PHOTON FACTORY, KEK)
- INSTABILITY FOR e^+ BEAM BUT NOT e^-
- BROAD SPECTRUM (NON-RESONANT ECE) (PRL 95)

DEC 85 : PSR (LANL) e-p INSTABILITY (R. MACEK)
D. NEUFFER PICTURE (~ 1991)

≳ 1985 CESR "ANOMALOUS ANTI-DAMPING" (J. ROGERS EXPLANATION ~1996 : e^- TRAPPING IN FIELD OF VACUUM PUMPS)

SIMULATION CODES : ≳ 1995 K. OHMI ; M. FURMAN
≳ 1997 F. ZIMMERMANN
M. BLASKIEWICZ , A. DANILOV, V. ALEKSANDROV
J. ROGERS
S. HEIFETS
Y. CAI
R. DAVIDSON , H. QIN
T. S. WANG "2-STREAM INSTABILITY"

ANALYTIC : G. STUPAKOV
L. VOS

DEDICATED e^- PROBES : K. HARKAY & R. ROSENBERG (ANL)
≳ 1997

BEAM - INDUCED MULTIPACTING

(RESONANT ECE)

(O. GRÖBNER, 1977)

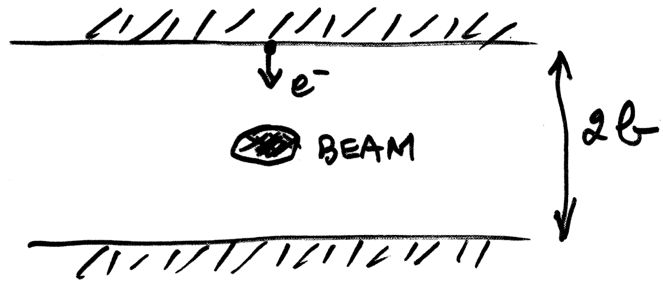

FLAT CHAMBER

e^- TRAVERSAL TIME = Δt (DUE TO ONE BUNCH PASSAGE
IMPULSE APPROX.)

SET $\Delta t = \frac{s_B}{c}$ s_B = BUNCH SPACING

$\rightarrow$ $s_B = \frac{b^2}{N r_e}$

N = PARTICLES / BUNCH
$r_e = 2.82 \times 10^{-15}$ m
$(= e^2/mc^2)$

(NEGLECTS IMAGE FIELDS, BUNCH LENGTH,
ENERGY SPREAD OF e^-, ...)

ECE SEEN AT

PHOTON FACTORY (PF)
BEPC
PEP-II
KEK-B
SPS
PS
APS
PSR

$\left.\begin{array}{l}\text{PEP-II}\\ \text{KEK-B}\end{array}\right\}$ LIMITING EFFECT

EXPECTED AT :

LHC
VLHC (STAGE 2)
NLC DR
CLIC DR
SNS (?)

Confidence level of ECE evidence

(PAC'01) (IMHO)

- Wild guess
- Guess
- Hunch
- Educated guess
- Vox populi
- The preponderance of evidence suggests that…
- What else could it be
- Smoking gun
- → Three unrelated witnesses in broad daylight swear that…

AT CENTER STAGE IS SEY

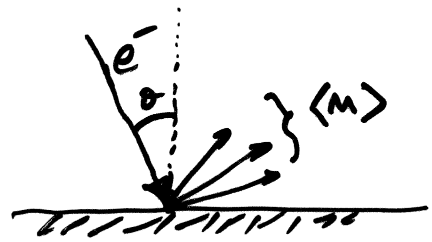

$$\delta(E,\theta) = \langle m \rangle$$

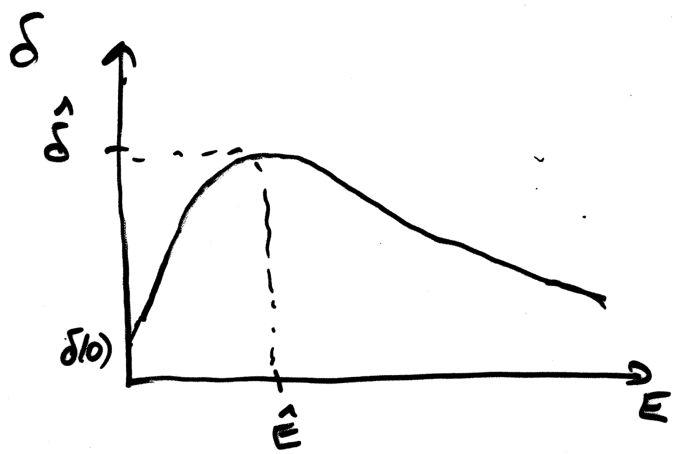

	$\hat{E}$	$\hat{\delta}$	$\delta(0)$
TiN	~250	1.1	?
Cu	~180-250	1.2-1.3	0.6 ?
Al_2O_3	~300	$\gtrsim 2.5$	?
SS	~250	~2.2	?

IN PRACTICE, WHAT COUNTS IS NOT δ BUT

$$\delta_{EFF.} = \int_0^\infty dE \int_0^{\pi/2} d\theta \; \delta(E,\theta) \times \rho(E,\theta)$$

$\rho(E,\theta)$ = SPECTRUM OF ELECTRONS HITTING THE CHAMBER WALL

$$\delta_{EFF} \begin{cases} > 1 \rightarrow \text{SEVERE} \\ < 1 \rightarrow \text{BETTER} \end{cases}$$

R. KIRBY & F. KING SLAC-PUB-8212

Contributions to the sample current from electron backscatter-bombardment of nearby surfaces (all graphite-coated) were measured at normal incidence using both RP and ZR methods. Secondaries generated at these surfaces have mostly very low energy and serve to strike and reduce the apparent yield of the sample. ZR curves need to be corrected (< 5%) for this effect. Primary electrons elastically scattering in the forward direction from the surface at grazing incidence were collected in a "black-hole" gridded structure behind the sample holder. The sample was moved laterally several electron beam diameters between successive angular measurements, to ensure that a previously-unbombarded area was used for the next SEY measurement.

XPS measurements were made on TiN-coated samples in a separate UHV system and then the samples were transferred to the SEY-measurement chamber. The SEY-measurement chamber has an Auger electron spectrometer (AES), which is used to check surface chemistry on a spot several mm away from the SEY-measurement area. Conditions in this system are similar to the LER, cleaned for UHV operation and unbaked with a pressure of one ntorr or so.

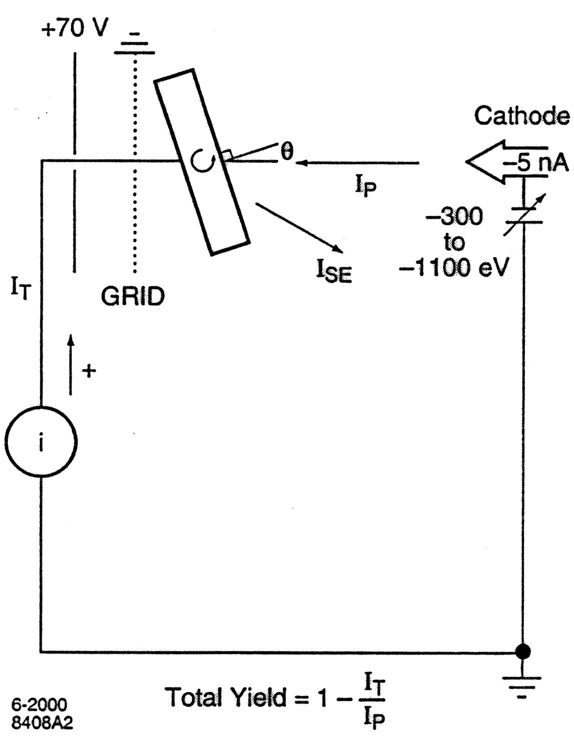

Figure 3. Circuit for zero retard yield measurements, angular beam incidence. The volume around the sample is at ground potential and field-free.

3. Results

3.1 General Comments

Figure 4 shows the unacceptably large (for beam chamber use) peak SEY of >2 of air-oxidized etched aluminum alloy. In fact, chemically removing residual carbon from the surface serves to increase the SEY by increasing the percentage of surface covered by high-yield aluminum oxide in place of lower yield carbon. Copper has a much lower yield and need not, for present machines at least, be coated with a SEY-lowering material. For aluminum alloy chambers and high-field components, TiN coating is frequently used. However, chambers are always exposed

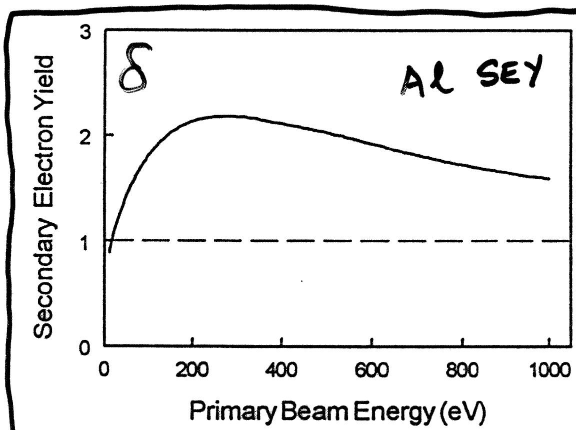

Figure 4. SEY of alkali-etched Al alloy in Figure 1.

to atmosphere following coating, which leads to a rise in the SEY of the coated surface. Such surfaces need to be "conditioned" in situ to restore a low SEY.

Conditioning of beam chambers, i.e., an in-situ reduction of the gas load from the chamber walls occurs by synchrotron light and electron bombardment. This process and its effect on the SEY of the walls is characterized as follows. The as-deposited/air-exposed SEY (e.g., TiN-coated aluminum alloy, Figure 5, inset) is mainly determined by the presence of a surface water and hydrocarbon layer [9]. Electron bombardment of this layer, the initial processing that occurs during machine comissioning, desorbs the gas layer and also results in electron-induced adsorption of carbon from carbon-containing residual-gas molecules. Water desorption and carbon deposition, amongst other processes discussed later in this paper, serve to reduce the peak SEY to near one (Figure 5, graph). This yield is close to the in-situ as-deposited TiN value [4]. The conditioning time can be reduced by glow discharge cleaning (GDC) of the chamber walls after machine assembly. Such ion sputter-removal of surface gas is much more efficient than photon/electron bombardment. Measurements of the SEY following simulated conditioning and GDC are included below.

R. KIRBY + F. KING SLACPUB-8212

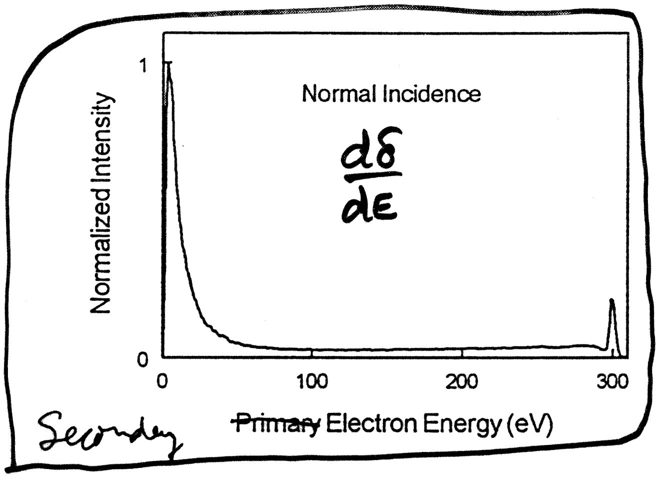

Figure 15. Collected electron energy distribution from TiN-coated Al alloy. The primary beam and analyzer axis were normal to the sample surface. The most probable secondary electron energy is 2.9 eV (8.4 eV FWHM).

The generated electron distribution curve (EDC) consists of true secondary, inelastic and elastically-reflected electrons. Forty eV is usually considered the high energy-pass cutoff for "true" secondary electrons. Relatively few primary electrons are backscattered elastically. The remainder of the generated spectrum consists of re-diffused primaries that have suffered loss events (ionizations, Augers, plasmons, etc.). The relative proportion of each kind of generated species is shown in Table I. An incidence energy of 300 eV was chosen because that is about the peak of the SEY and, hence, the most efficient for total secondary electron production. At lower primary energies, a progressively larger fraction of the distribution will be elastic [11]. The emitted electron angular spectrum will be cosine but peaked for backscattered elastics.

θ	0–40 eV	40–295 eV	295–310 eV
0°	58.9 %	36.6 %	4.5 %
82.5°	56.8 %	38.9 %	4.3 %

Table I. Normalized EDC intensity areas at normal (0°) and grazing (82.5°) primary electron incidence angle θ.

At a grazing incidence of 82.5°, the EDC still looks very similar to Figure 15 but now with the most probable energy at 2.7 eV (7.1 eV FWHM). Unlike normal incidence, more primaries will stay within the escape depth of generated low-energy secondaries, i.e., grazing incidence increases the SEY. Unfortunately, the energy analyzer has its axis along the primary beam direction, resulting in an off-sample-normal collection slit. The relative proportion of each kind of generated species is about the same (Table I), however, suggesting that the TiN surface roughness is sufficient to homogenize the secondary emission over all incidence angles.

3.5 The Secondary Yield Of Other Materials

The SEY of some materials used for beam vacuum chamber construction (and graphite, for reference) are plotted in Figure 16. The surfaces were Ar-sputtered (~1×10^{17} ions-cm^{-2}) to remove most, but not all, surface contamination, as determined by Auger electron spectroscopy. Remaining carbon levels were in the 1-5 atomic per cent range. The yields of Figure 16 are those expected for beam vacuum chambers that have been glow-discharge cleaned after assembly and pumpdown.

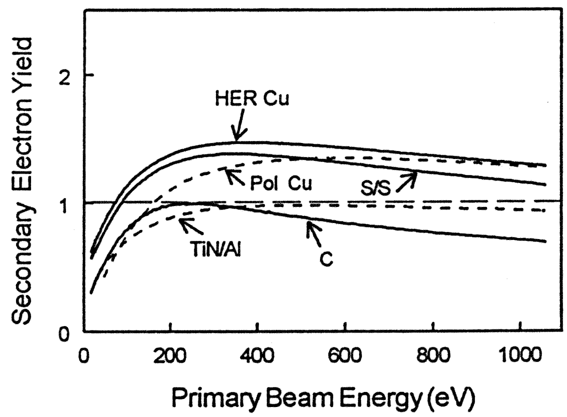

Figure 16. SEY of some materials used in accelerator/storage ring construction. Graphitic carbon is included as a measurement reference.

The yield of sputter-cleaned TiN is consistent with previous work for as-deposited, not exposed to air, films [4]. The result for polished copper ("Pol Cu") shows a shift of the peak SEY to higher primary energy, probably due to less electron-scattering (SEY-lowering) surface disorder.

4. Discussion

4.1 Primary Angle Dependence of SEY Peak Yield

SEY theory predicts that the normalized yield δ/δ_0, where δ_0 is the SEY maximum at normal incidence, should vary as $1/\cos\theta$ [12]. Figures 17 and 18 show that the experimental data from TiN/Al or Cu do not match theory for the simple case, $E_P = E_{MAX}$, (i.e., the yield is not tending toward large values as θ approaches grazing angles) and, incidentally, appears independent of conditioning (Figure 17) as well. E_P is the primary electron energy and E_{MAX} is the primary electron energy corresponding to the maximum SEY, δ_0, at normal incidence.

Secondary electron emission

- main quantity of interest is the secondary emission yield (SEY) δ:
  - δ=average number of ejected electrons per incident electron
    - function of: incident energy E_0, incident angle θ_0 and surface material
  - model parametrized to fit data by R. Kirby and F. King (SLAC) for TiN-coated extrusion sample

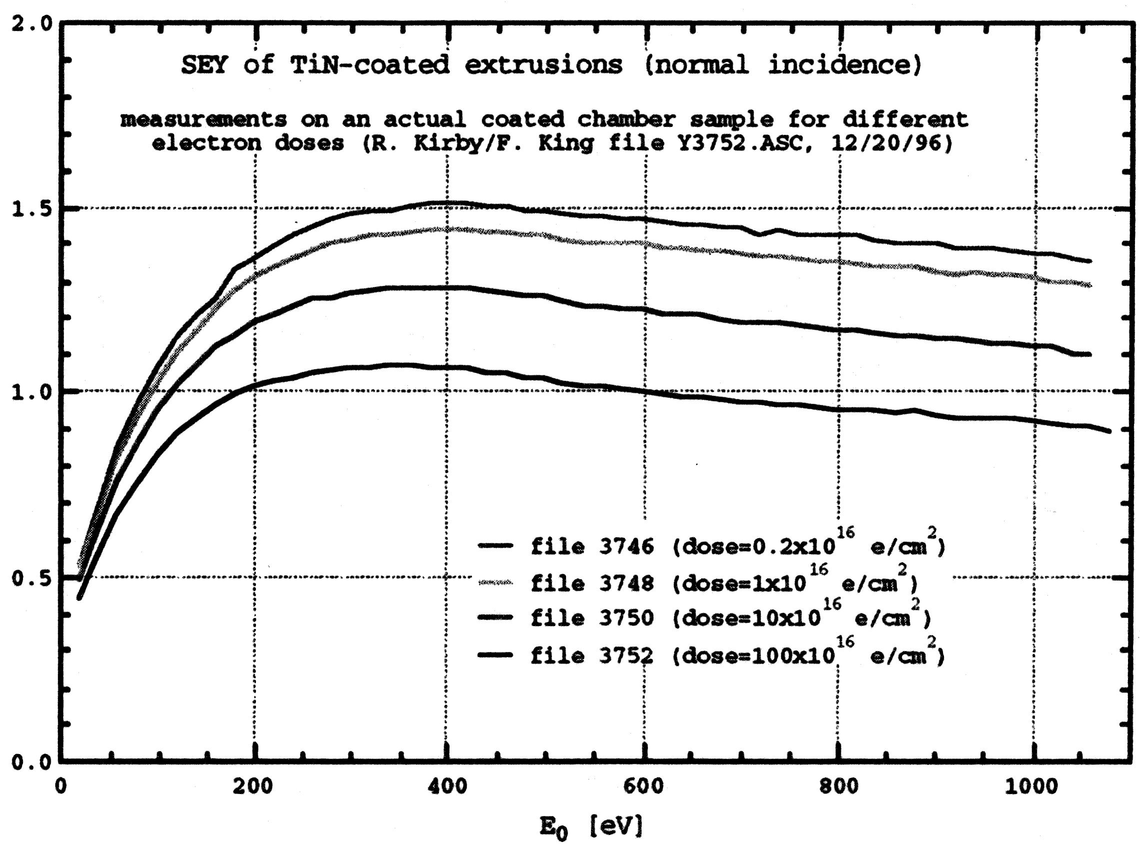

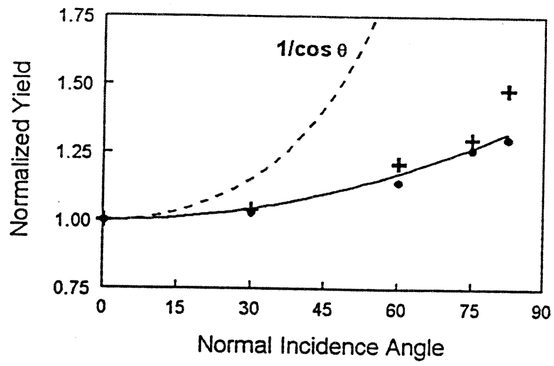

Figure 17. Normalized peak yields from TiN/Al (Figures 6 (●) and 8 (+)) vs. primary beam incidence angle, at E_{MAX} =440 and 389 eV, respectively. The curve fit is exp [0.32 (1-cos θ)].

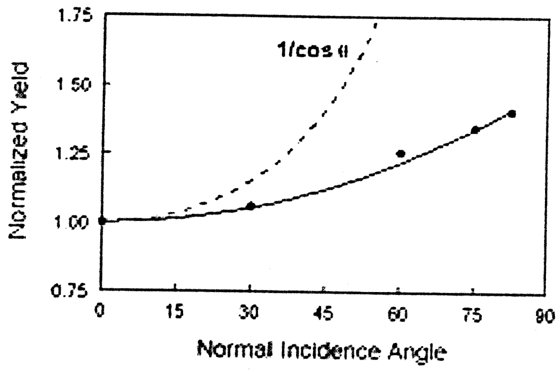

Figure 18. Normalized peak yields from HER copper (Figure 13) vs. primary beam incidence angle, at E_{MAX} =675 eV. The curve fit is exp [0.40 (1-cos θ)].

The lack of agreement with theory begins to occur far from grazing incidence, so this does not appear to be a surface-only related phenomenon. In fact, the surface finishes of the TiN/Al and Cu are quite different. However, as the primary beam angle moves toward grazing incidence, an ever-increasing fraction of primaries will exit the surface, in the forward direction, before losing their full energy to secondary electron production [13]. A simple phenomenological explanation, due to Bruining [14], accounts for the exponential dependance of Figures 17 and 18. Suppose X_m is the average depth (Figure 19) at which N_s secondary electrons are generated at normal primary beam incidence.

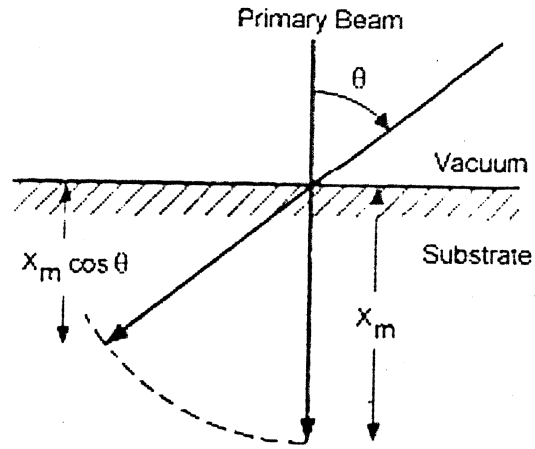

Figure 19. Schematic diagram [14] showing the secondary electron generation depth, X_m, as a function of primary electron incidence angle, θ.

Then the escape probability depends on secondary electron absorption α, and the SEY is given by

$$1)\quad \delta_0 = N_s\, e^{-\alpha X_m}$$

At other than normal incidence, the yield is

$$2)\quad \delta_\theta = N_s\, e^{-(\alpha X_m \cos\theta)}$$

Combining, the normalized yield as a function of primary incidence angle is given by

$$3)\quad \delta_\theta / \delta_0 = e^{\alpha X_m (1-\cos\theta)}$$

which dependence fits the experimental data very well, as shown in Figures 17 and 18.

4.2 Electron Conditioning - LER

Figure 20 shows the air-exposed TiN-coated Al peak yields, as a function of electron dose, for three different samples, all pre-exposed to ambient atmosphere. The dosing and SEY measuring beams were normal to the surface. As an aside, others [15] have made such measurements to higher dose and shown that the peak yield levels off at approximately 1×10^{18} electrons cm^{-2}.

MOTIVATION

- ELECTRON CLOUD CODES HAVE BEEN DEVELOPED FOR ~ 6 YEARS NOW.

- USED TO PREDICT ELECTRON CLOUD EFFECTS AT VARIOUS MACHINES, e.g. PEP-II, LHC, VLHC, APS, PSR, SPS, ...

- ~~IN PARTICULAR, LBL CODE~~

- DURING THE PAST ~ 4 YEARS, SPECIALIZED e^- DETECTORS HAVE BEEN BUILT + DEPLOYED AT APS, PSR, BEPC

- COMPARE SIMULATION RESULTS AGAINST CONTROLLED MEASUREMENTS AT APS

  SPECIFICALLY:

  * ELECTRON CURRENT AT THE WALLS
  * APS WITH e^+ BEAMS
  * VARY BUNCH SPACING, FIXED TOTAL CURRE

APS VACUUM CHAMBER
AND e^- DETECTORS
(K. HARKAY + R. ROSENBERG)

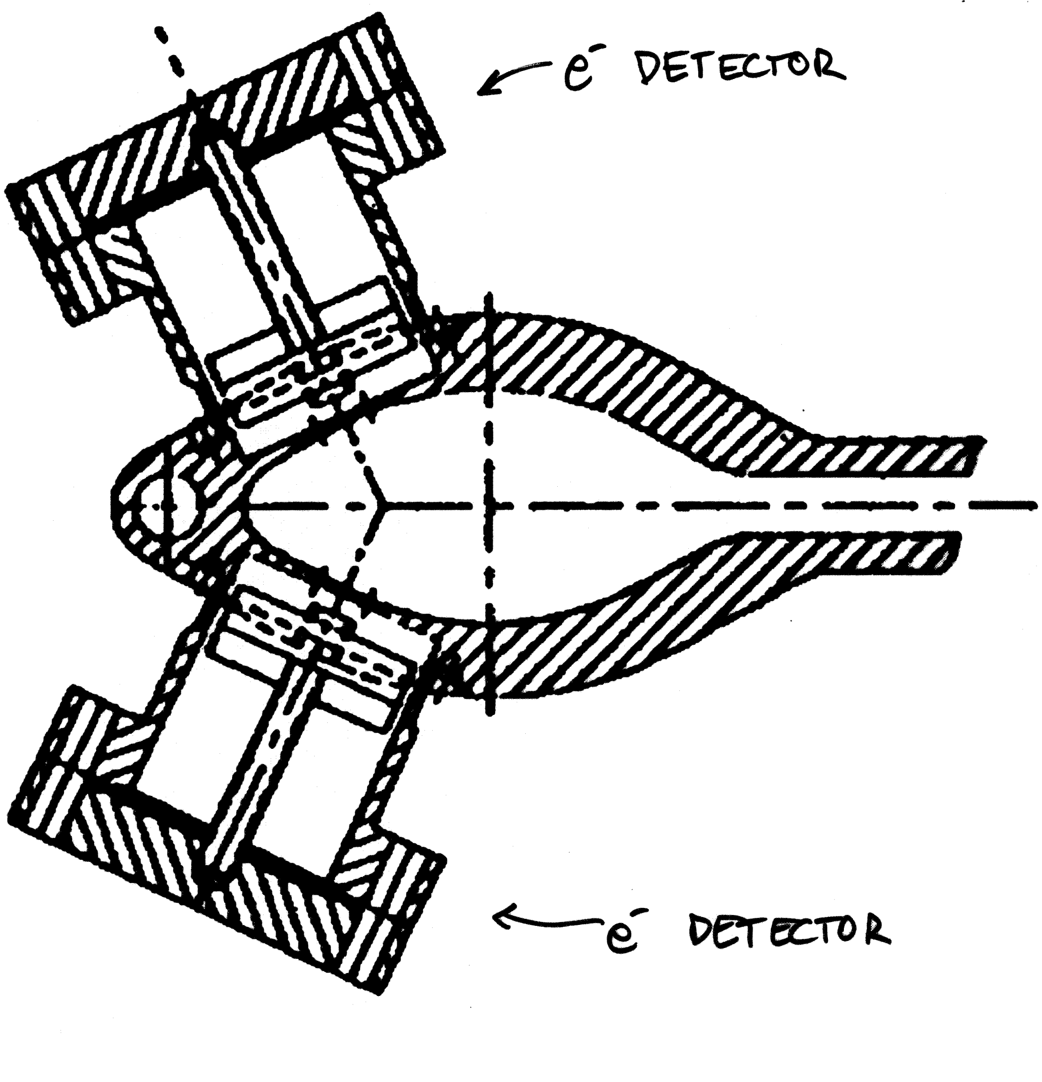

FEATURES OF THE LBNL SIMULATION CODE

- BEAM IS NON-DYNAMICAL
- ELECTRONS IN THE CLOUD ARE FULLY DYNAMICAL
- ELECTRONS GENERATED BY
  * PHOTOEMISSION
  * SECONDARY ELECTRON EMISSION
  * RESIDUAL GAS IONIZATION
- CAN SIMULATE:
  * FIELD-FREE REGION
  * DIPOLE FIELD
- 3D ELECTRON KINEMATICS
- 2D (TRANSVERSE) FORCES
- SPACE CHARGE
- IMAGE CHARGES
- ELLIPTICAL VACUUM CHAMBER
- POSSIBLE ANTECHAMBER

+

$$\left.\begin{array}{l}\delta = \text{SECONDARY EMISSION YIELD} \\ \dfrac{d\delta}{dE} = \text{SECONDARY ENERGY SPECTRUM}\end{array}\right\} \text{DETAILED INPUT MODEL}$$

DATA FOR SEY FROM SLAC MEASUREMENTS (R. KIRBY)

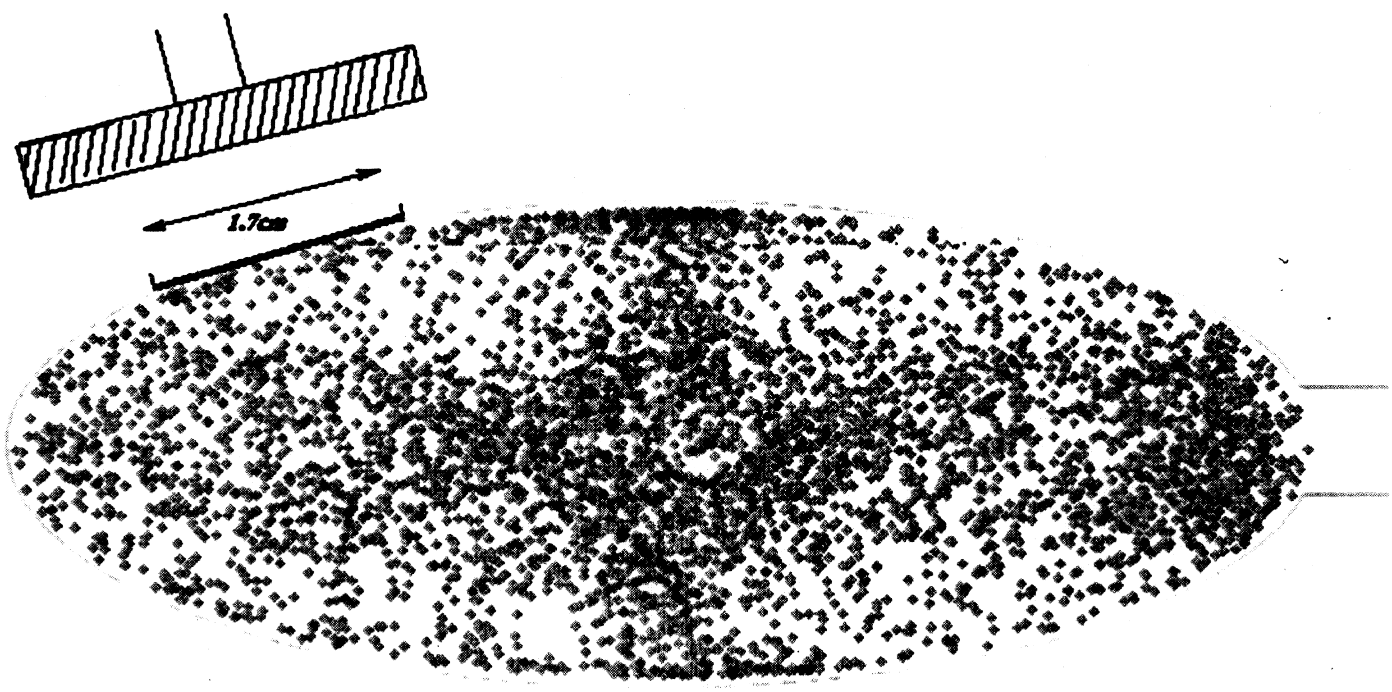
1.7cm

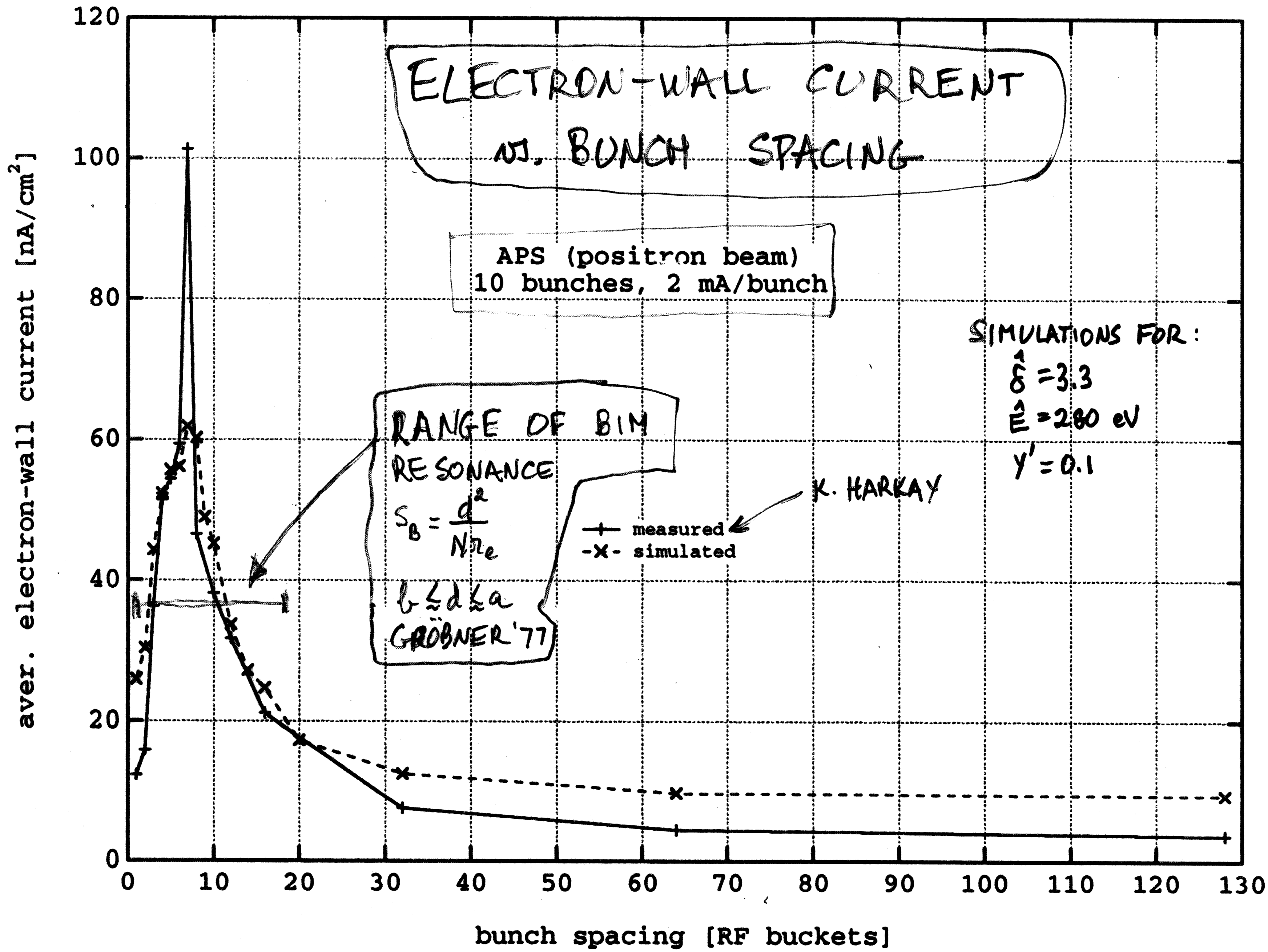

ELECTRON-WALL CURRENT
vs. BUNCH SPACING
APS (positron beam)
10 bunches, 2 mA/bunch
SIMULATIONS FOR:
$\hat{\delta} = 3.3$
$\hat{E} = 280$ eV
$y' = 0.1$
RANGE OF BIM
RESONANCE
$s_B = \frac{d^2}{N r_e}$
$b \lesssim d \lesssim a$
GRÖBNER '77
measured
simulated
K. HARKAY
aver. electron-wall current [nA/cm^2]
bunch spacing [RF buckets]
0
20
40
60
80
100
120
10
30
50
70
90
110
130

SIMULATIONS + MEASUREMENTS AT PSR

- R+D PROGRAM TO UNDERSTAND PSR INSTABILITY
  - EST. ~ FEB 2000, FUNDED BY SNS
  - LANL, BNL, LBNL, PPPL, ORNL, ANL
  - P.I. R. MACEK
  - TERMINATED ~ DEC 2000 (FORMALLY)
  - WORK CONTINUES
  - POST-DOC MAURO PIVI HIRED UNDER THIS PROGRAM (LBNL)
  - COMBINATION OF THEORY, SIMULATIONS + EXPERIMENTS
  - INSTALLED ANL e^- DETECTORS IN PSR (HARKAY - ROSENBERG)

TRAILING-EDGE MULTIPACTING

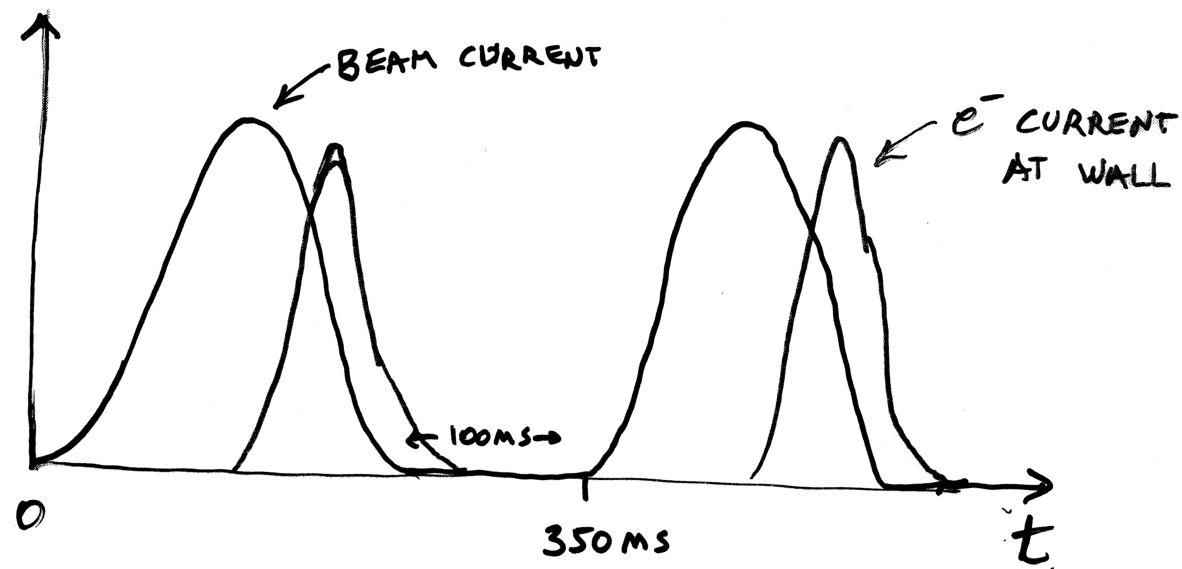

ELECTRONS "SUCKED IN" DURING LEADING EDGE
THEN RELEASED DURING TRAILING EDGE

$C = 90$ m
$N = 5\times10^{13}$
$T_{BUNCH} \simeq 250$ ns
$T_{GAP} \simeq 100$ ns

SIMULATIONS:
BLASKIEWICZ, ALEKSANDROV, DANILOV

MAIN SOURCE OF e^- : LOST PROTONS HITTING THE CHAMBER
$\sim 10^{-6}$ p/p/TURN
$\sim 100\ e^-/p$

PSR beam current and electron-detector signal: (MEASUREMENT)

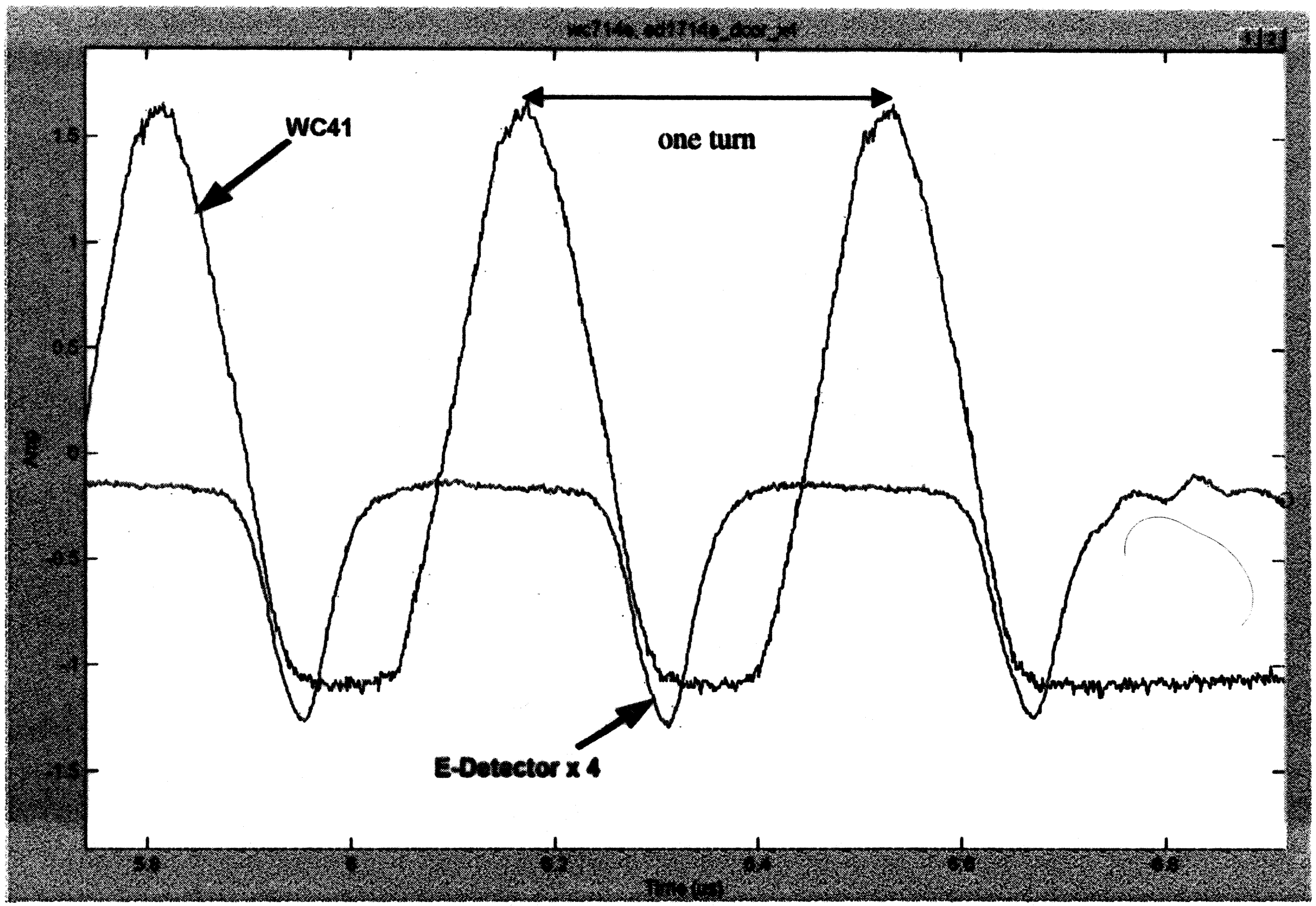

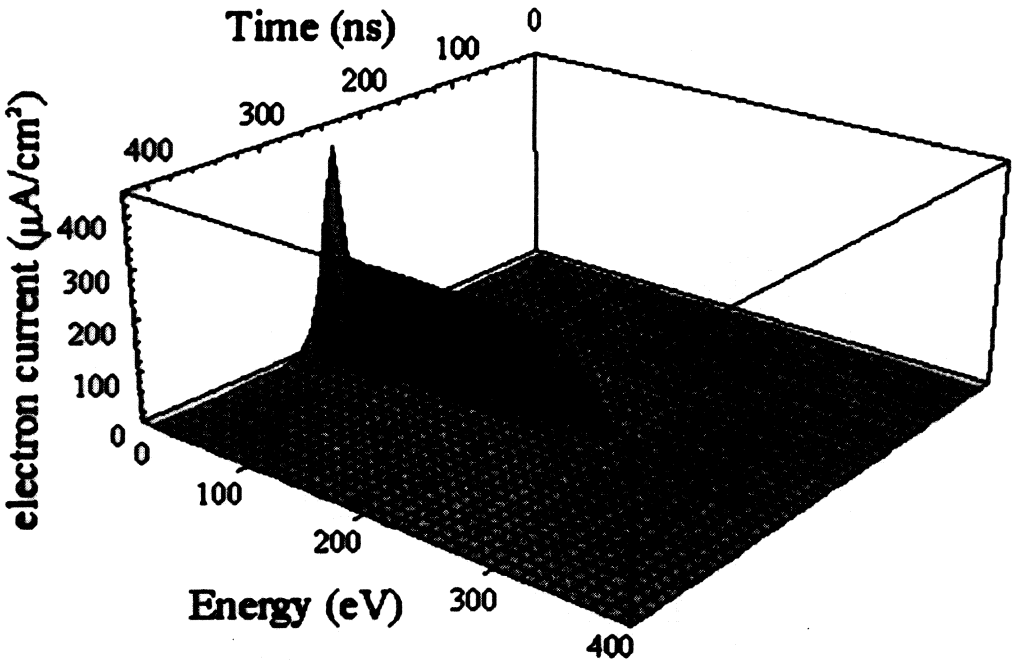

PSR: SIMULATED

CUMMULATIVE-ENERGY SPECTRUM

(M. FURMAN, M. PIVI, PAC'01)

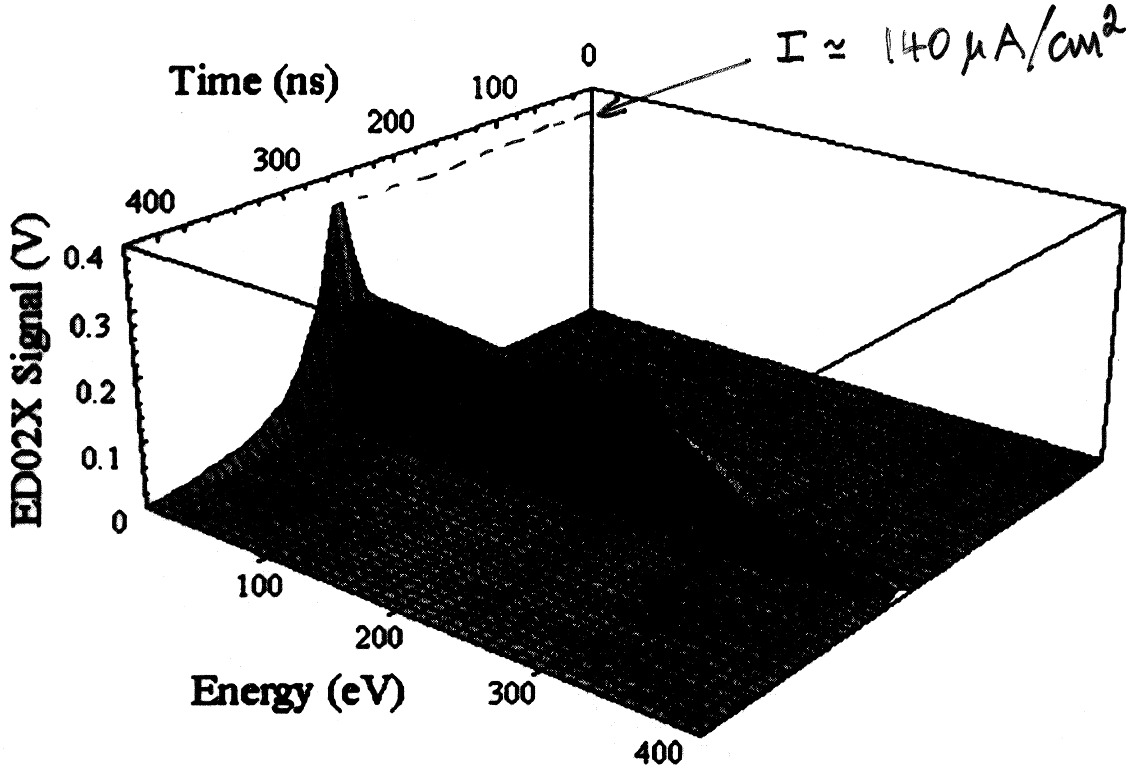

PSR : MEASURED

CUMMULATIVE-ENERGY SPECTRUM

(COURTESY R. MACEK)

NEW SIMULATION RESULTS FOR THE ELECTRON-CLOUD EFFECT AT THE PEP-II POSITRON RING

Y. CAI, S. HEIFETS, J. SEEMAN (SLAC)

M. FURMAN, M. PIVI (LBNL)

FRI. 6/22/01
PACO1

ACKNOWLEDGMENTS: R. KIRBY, N. HILLERET, I. COLLINS, V. BAGLIN, F. ZIMMERMANN, O. GRÖBNER, O. BRÜNING, G. LAMBERTSON, K. KENNEDY, K. OHMI, J. ROGERS, F. RUGGIERO, M. ZISMAN, V. BAGLIN, K. HARRAY

RELATED PRESENTATIONS AT PACO1:

TPPH126 ₹
WOAA003
TPPH100
ROPB001
⋮

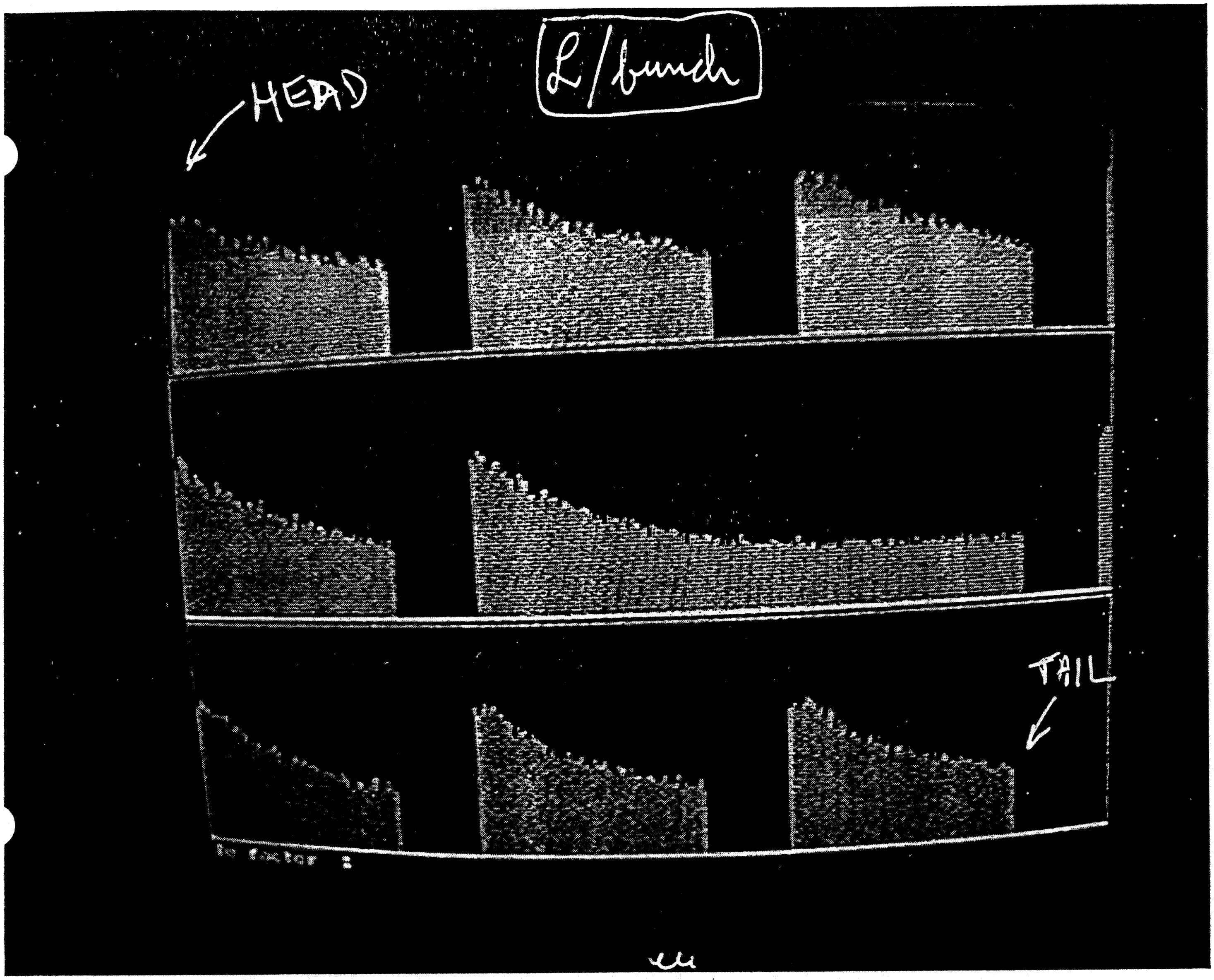

This is *one* turn

obviously not BB problem
probably not RF transient

data taken July 2000 (most likely)

PEP-II
Bunch By Bunch
Luminosity

(J. SEEMAN)

GRADUAL $\mathcal{L}$ DECREASE ALONG BUNCH TRAIN IS DUE TO e^+ BEAM BLOWUP DUE TO ELECTRON CLOUD

STRONG EVIDENCE FROM:

- PRESSURE RISE vs. I (FILL PATT. DEPENDE
- BENEFICIAL EFFECT OF SOLENOIDAL FIELD
- $\sigma_x + \sigma_y$ BLOWUP vs. I (SYNCHROTRON LIGHT INTERFEROMETER)

SIMULATIONS WERE DONE BY TWO CODES:

1) LBNL CODE → DETERMINE ELECTRON-CLOUD DENSITY n_e

2) SLAC CODE: INPUT n_e → DETERMINE BEAM BLOWUP

---

* FEATURES OF THE LBNL CODE:
  - ARBITRARY FILL PATTERN
  - RIGID BUNCHES
  - PHOTOELECTRONS
  - SECONDARY ELECTRON EMISSION
  - VAC. CHAMBER GEOMETRY, INCL. ANTECHAMBER
  - 3D ELECTRON KINEMATICS
  - 2D (TRANSVERSE) FORCES
  - SPACE-CHARGE
  - IMAGE CHARGES

PEP-II LER SIMULATION: e^- DENSITY vs. TIME ($N = 5\times10^{10}\ e^+$/BUNCH)

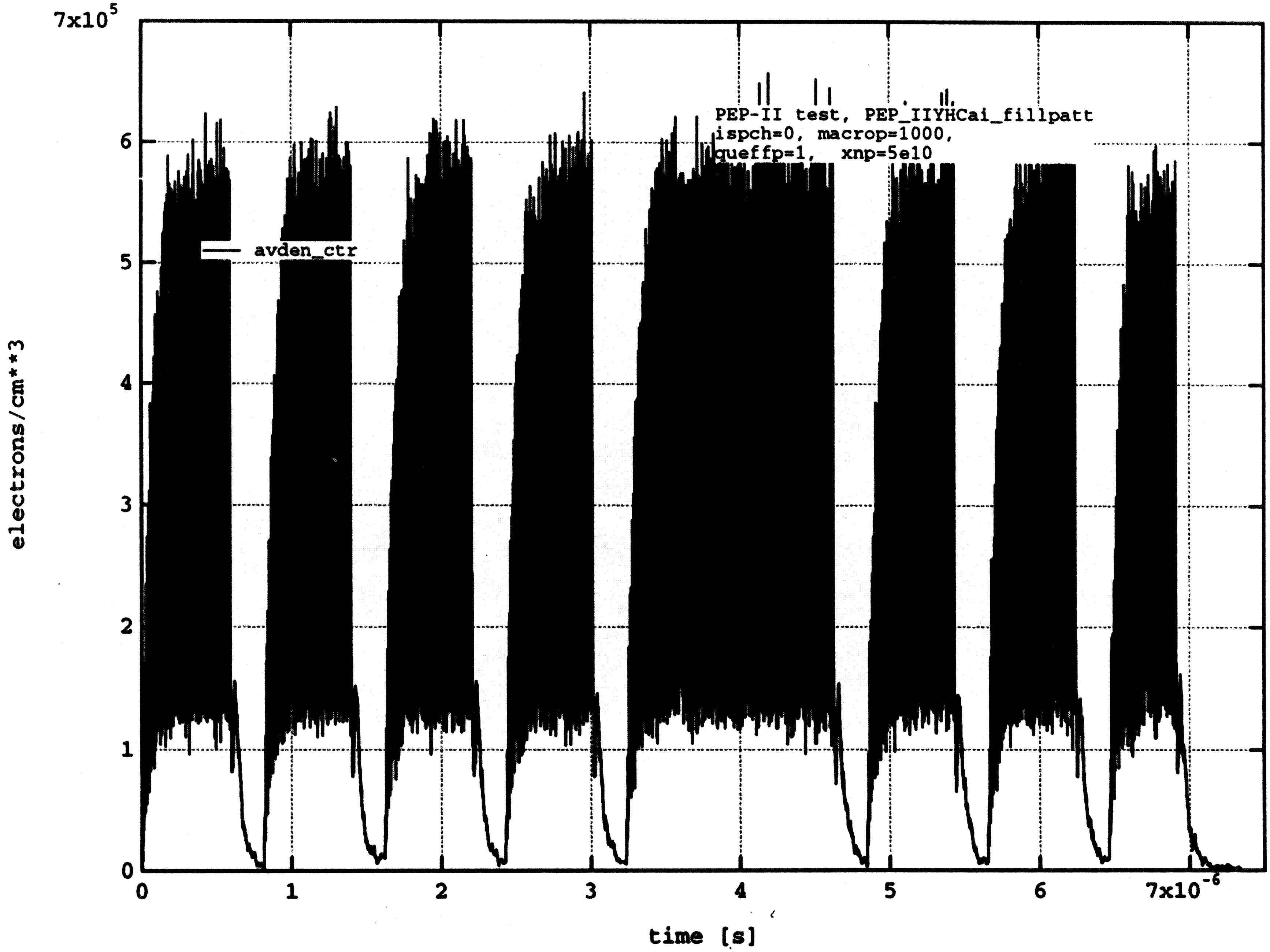

FEATURES OF THE SLAC CODE

- MODEL: OHMI & ZIMMERMANN (PRL 85, 3821, 2000)
- ELECTRON CLOUD IS STATIC, LUMPED AT ONE POINT IN THE RING
- POSITRON BUNCH IS DYNAMICAL (MACROPARTICLES, LONGITUDINALLY SLICED)
- CHROMATICITY
- 3D (INCL. SYNCHROTRON MOTION OF POSITRONS)
- C++

E	BEAM ENERGY	3.1 GeV
β_x	AV. β_x	9.37 m
β_y	AV. β_y	12.47 m
σ_x	AV. σ_x	0.5 mm
σ_y	AV. σ_y	0.14 mm
σ_z	RMS BUNCH LENGTH	1.3 cm
σ_p/p	MOM. SPREAD	7.7×10^{-4}
ν_x	H. TUNE	0.649
ν_y	V. TUNE	0.564
ν_s	SYNCHR. TUNE	0.0251
N_p	# e^+/BUNCH	1×10^{11}
σ_x^c	e-CLOUD σ_x	6 mm
σ_y^c	e-CLOUD σ_y	3 mm
N_s	# SLICES	1024
N_m	# MACROP./BUNCH	10240
ξ_x, ξ_y	CHROMATICITY	(VARIABLE)
n_e	e^- CLOUD DENSIT	(VARIABLE)

PEP-II ECE SIMULATIONS
(YUNHAI CAI)

NOMINAL
$\sigma_x^{(0)} = 0.5$ mm
$\sigma_y^{(0)} = 0.14$ mm
$\xi_x = \xi_y = 0$

$\cancel{\Sigma_y \sqrt{\sigma_y^2 + \langle y^2 \rangle}}$ ~~vs. TIME~~

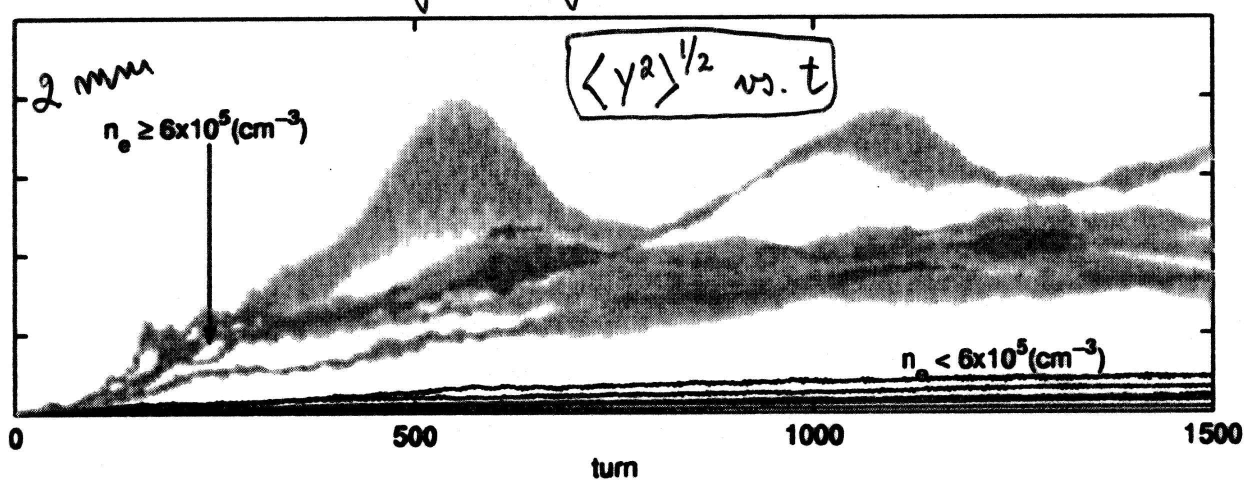

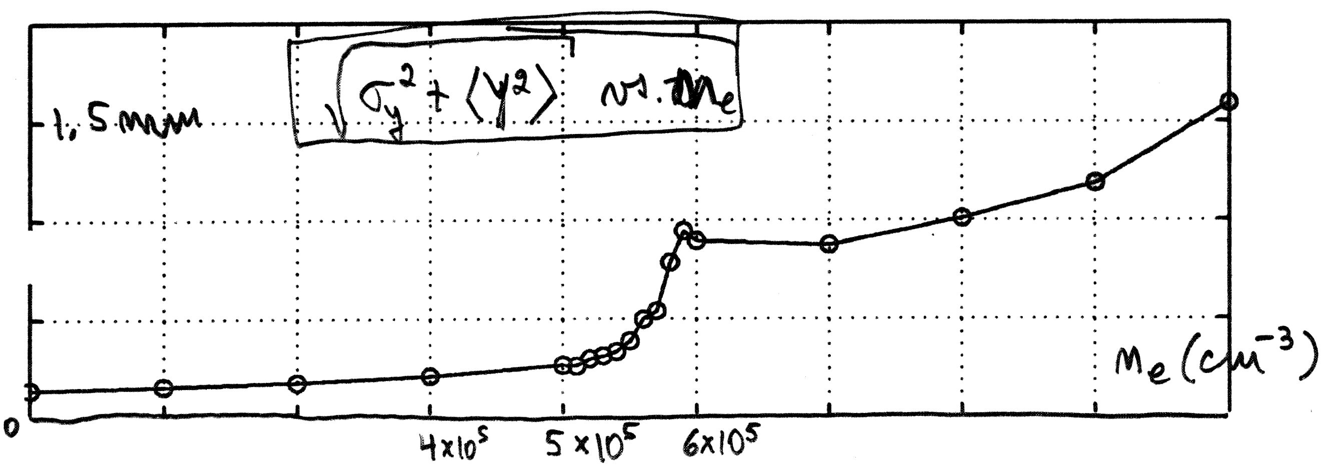

PEP-II ECE SIMULATIONS

(YUNHAI CAI)

FIX: $n_e = 8 \times 10^5\ \mathrm{cm}^{-3}$, $\xi_x = 0$

(NOMINAL: $\sigma_x^{(0)} = 0.5$ mm , $\sigma_y^{(0)} = 0.14$ mm)

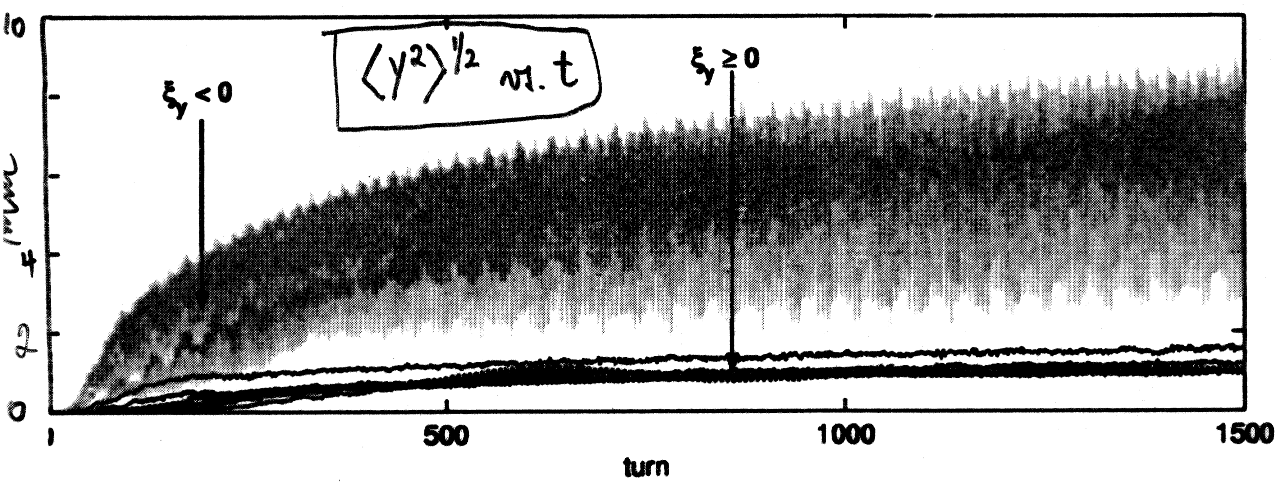

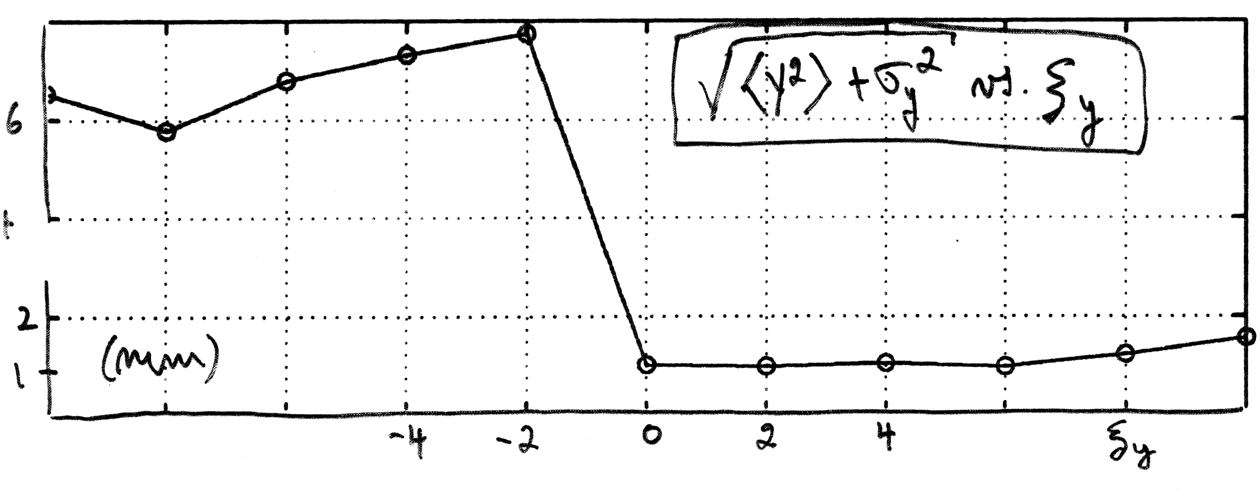

CONCLUSIONS

- CLEAR THRESHOLD BEHAVIOR OF σ vs. n_e AT $n_e \sim 5\times10^5$ e/cc
- CLEAR BENEFICIAL EFFECT FROM $\xi_y > 0$
- RESULTS ARE PRELIMINARY
- NEED ~~TO~~ A BETTER DETERMINATION OF n_e
  (TAKE INTO ACCOUNT VARIOUS ELEMENTS ALONG THE RING)
- RECONCILE WITH OBSERVATIONS

ECE IN LHC: POWER DEPOSITION

F. ZIMMERMANN
O. BRÜNING
G. RUMOLO
M. FURMAN
M. PIVI

R = PHOTON REFLECTIVITY

POWER DEP. IN LHC ARCS
IN W/m

R	$\delta(0)$	$\hat{\delta}$	DRIFT	BEND
0.1	0	1.9	5.2	2.3
0.1	0	1.1	0.67	0.03
0.1	0.6	1.9	14.7	5.44
0.1	0.6	1.1	1.9	0.3
0.05	0.6	1.9	14.7	3.54
0.05	0.6	1.1	1.9	0.22

(F. ZIMMERMANN, CHAMONIX 2001)

ECE AT PEP-II + KEK-B

~~ECM~~ * BEAM BLOWUP (SINGLE-BUNCH EFFECT)

FROM e^- SUCKED INTO THE BUNCH

SIMULATIONS : Y. CAI
F. ZIMMERMANN } PRL 2000
K. OHMI

~ HEAD-TAIL EFFECT

~~PEP-II~~ :

* ALSO POSSIBLE : COHERENT MULTIBUNCH INSTABILITY
(→ CONTROLLED BY FEEDBACK)

* NONLINEAR PRESSURE RISE
  - DEPENDS ON: LOCATION
    BUNCH CURRENT
    FILL PATTERN

IN CONCLUSION...

1) AVOID BIM (ADJUST s_B, N) IF $\delta_{EFF} \gg 1$

2) CHOOSE MATERIALS / COATINGS WITH LOW SEY

3) " " " " " Y
(Y = PHOTOELECTRIC YIELD)

4) IF SYNCHROTRON RADIATION HAS $E_{CRIT} \gtrsim 4$ eV
→ USE ANTECHAMBER

5) PHOTON REFLECTION COEFF. R MAY BE IMPORTANT

6) IF s_B "LARGE" (OR IF THERE IS A LONG GAP) → OTHER DETAILS OF SEY BECOME IMPORTANT:

→ LHC 25ns

↳ PSR, 100ns

$$E_s = \sum_i E_i$$

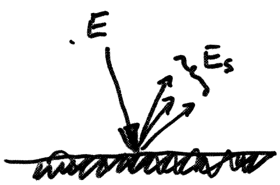

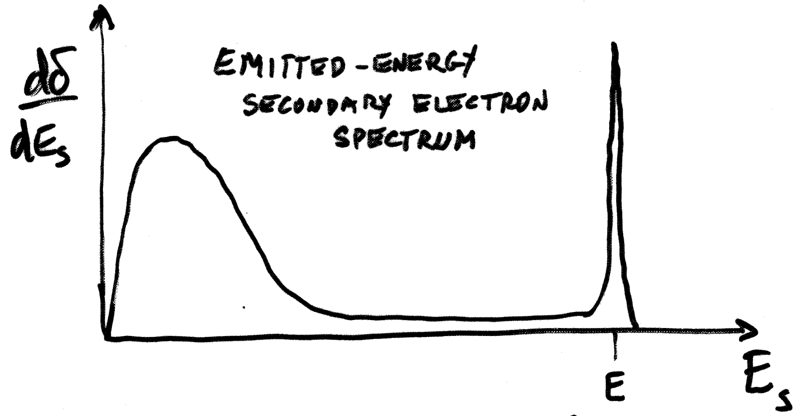

E = INCIDENT (PRIMARY) ENERGY

REMEDIES

1) WEAK SOLENOIDAL FIELD (PEP-II, KEK-B)
$B \sim 20-30$ G

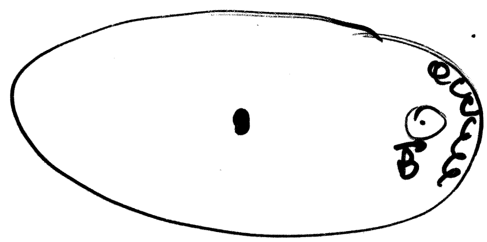

WORKS "VERY WELL"

(TRAP ELECTRONS NEAR WALLS)

2) LOW-SEY COATING (PEP-II) (TiN)
(IF ALUMINUM)

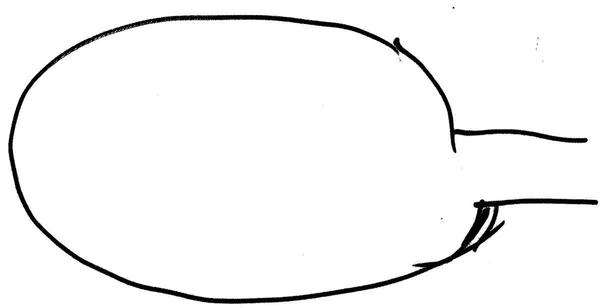

3) ANTECHAMBER (PEP-II)
EXTRACT ~99% OF S.R. PHOTONS

4) SAWTOOTH SURFACE (LHC, KEK-B (?))

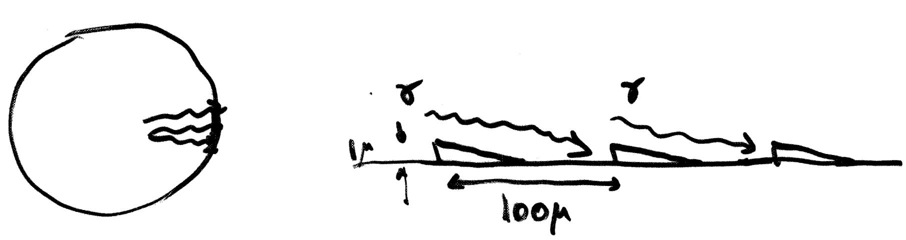

(DECREASE R + Y)

IMPORTANT RESEARCH NEEDED:

- MEASUREMENTS OF SEY $\delta(E)$,
  ESPECIALLY $\hat{\delta}$, $\hat{E}$, AND δ FOR $E \lesssim 10\,eV$
- MEASUREMENTS OF EMITTED-ENERGY SPECTRUM

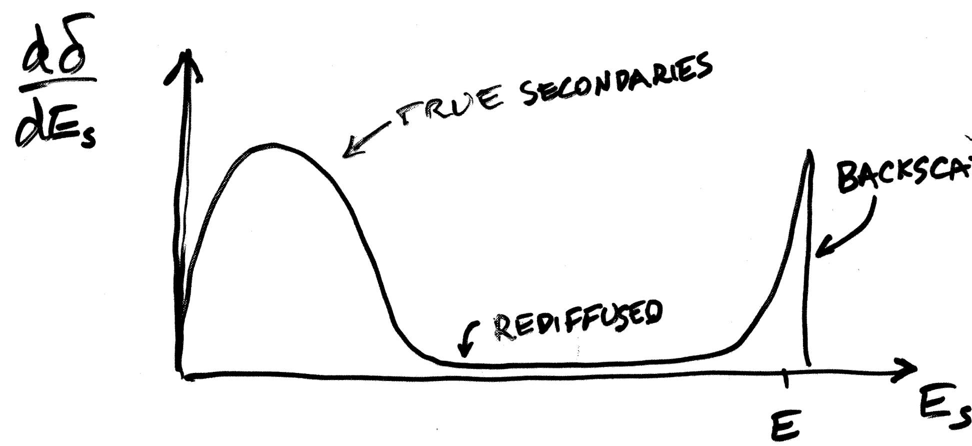

$$\delta(E) = \int_0^E dE_s \frac{d\delta}{dE_s}$$

- FURTHER CALIBRATE SIMULATION CODES VS. MEASUREMENT
  ESP. POWER DEPOSITION (SPS PROGRAM)